

Cost-effective Noninvasive 2.4 GHz Microwave Blood Glucose Sensor

Ja-Hao Chen* and Keng-I Lai

Department of Communications Engineering, Feng Chia University,
No. 100, Wenhwa Rd., Seatwen, Taichung 407102, Taiwan (R.O.C.)

(Received August 28, 2023; accepted March 26, 2024)

Keywords: noninvasive, blood glucose sensor, portable, metamaterial cells, cost-effective

A cost-effective noninvasive 2.4 GHz microwave blood glucose sensor is designed and implemented in this study. The special feature of the system is that it can operate independently without any other equipment, and the system is small in size and easy to carry. When the system is powered on and the ring finger is placed on the sensor, the blood glucose level (BGL) can be determined. The system is easy to operate and can be used continuously. For the system, a special sensor element with metamaterial cells and a specific RF-DC rectifier circuit are designed and implemented. An algorithm that can calculate BGL from the sensing voltage generated by detecting the fingertip and programmed to run in the embedded system is developed. Compared with BGL detected by a commercially available invasive blood glucose sensor, the detection error of the proposed sensor is less than 2%. The proposed noninvasive 2.4 GHz microwave blood glucose sensor is very simple and inexpensive, and the measurement results are very close to those of commercially available sensors.

1. Introduction

According to the International Diabetes Federation (IDF), there are approximately 537 million adults (20–79 years) worldwide in 2021 living with diabetes, and this will rise to 643 million by 2030 and 783 million by 2045. Over half of them are unaware that they have the disease, leading to an increase in burden on healthcare systems.⁽¹⁾ Diabetic patients can use invasive glucose monitors (glucometers) to independently check their blood glucose levels. Invasive glucose monitoring is currently the mainstream method for self-monitoring blood glucose. However, the pain, cost, and inconvenience associated with current self-monitoring technologies often lead patients to not comply with regularly performing sufficient daily measurements, thus limiting the benefits of self-monitoring the blood glucose level (BGL). Accordingly, there has been a demand for noninvasive pain-free glucose monitors to guarantee more affordable, careful, and comfortable control of BGL.⁽²⁾

In the previous years, many noninvasive techniques have been published. Such techniques require samples of saliva,⁽³⁾ urine,⁽⁴⁾ and tears⁽⁵⁾ for monitoring blood glucose.

*Corresponding author: e-mail: chiahaoc@fcu.edu.tw
<https://doi.org/10.18494/SAM4626>

Other techniques using reverse iontophoresis,⁽⁶⁾ bio-impedance spectroscopy,⁽⁷⁾ and ultrasound⁽⁸⁾ were investigated. However, these techniques are not widely used because they are not portable and have issues such as unstable measurement and long measurement time. Recently, some researchers have proposed a technique based on electromagnetic sensing technology for the noninvasive monitoring of BGL, and this technique has been shown to be promising.^(9,10) Some microwave components (such as antennas,⁽¹¹⁾ filters,⁽¹²⁾ transmission lines,^(13,14) or waveguides⁽¹⁵⁾) cooperate with vector network analyzers (VNAs) to sense BGL. However, microwave sensing technologies rely on costly and bulky VNAs, making them unportable, expensive, and inconvenient.

More recently, Omer *et al.* and Gelosi *et al.* have proposed the microwave sensor noninvasive monitoring of BGL without VNA measurement.^(16,17) In Omer *et al.*'s study, a low-cost portable planar microwave sensor for the noninvasive monitoring of BGL using a radar system instead of the previous VNA measurement was proposed.⁽¹⁶⁾ They designed four cells of hexagonal complementary split-ring resonators (CSRRLs) as a sensor. When an examiner's fingertip is placed onto the sensor, the output signal of the sensor is transmitted to a PC through the radar system and BGL is calculated by applying the principal component analysis (PCA) feature extraction algorithm. In Gelosi *et al.*'s study, a noninvasive portable device for measuring BGL with an embedded system and computer software is presented.⁽¹⁷⁾ These two proposed sensors are possible candidates for the noninvasive monitoring of glucose levels in diabetes patients as evidenced by the preliminary results of a proof-of-concept *in vivo* experiment that involved monitoring an individual's BGL by placing his fingertip onto the sensor. However, these two BGL sensing systems still require a laptop or desktop PC for measurement, and they cannot achieve a scenario where the inspector can easily carry them for measurement at any time.

In this study, a low-cost portable noninvasive microwave blood glucose sensor is designed and implemented. The BGL sensor has a unique design, having a transmission line on the FR4 substrate with 2.4 GHz metamaterial cells on the backside. When the fingertip is placed on the sensor, the output signal frequency response of the sensor is varied. An embedded system is used to recognize the variations of the sensor signal to estimate BGL, which is then displayed on the screen. The overall sensor device is small ($12 \times 17 \times 8 \text{ cm}^3$). The proposed device can operate independently without PCs and VNAs, and the inspector can easily carry it for measurement at any time.

2. Sensing System Operation

The overall structure of the BGL sensor system is shown in Fig. 1. The proposed system includes a microwave/RF signal generator, a sensor, an RF-DC rectifier, an amplifier, an embedded system, and a monitor. The signal generator can generate a 2.4 GHz high-frequency signal and import it into the sensor. When the fingertip touches the sensor, BGL in the finger affects the insertion loss frequency response of the RF signal. The affected RF signal is converted to DC voltage with BGL information by the RF-DC rectifier. The amplifier module

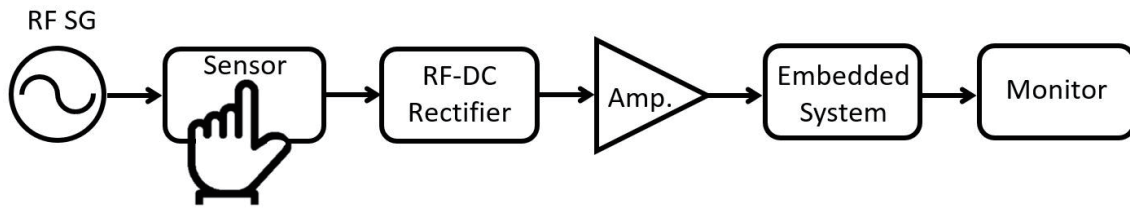


Fig. 1. Proposed BGL sensor system structure diagram.

(Amp.) as shown amplifies the DC voltage and feeds it into the embedded system. The embedded system displays the BGL information on the monitor by recognizing the DC voltage.

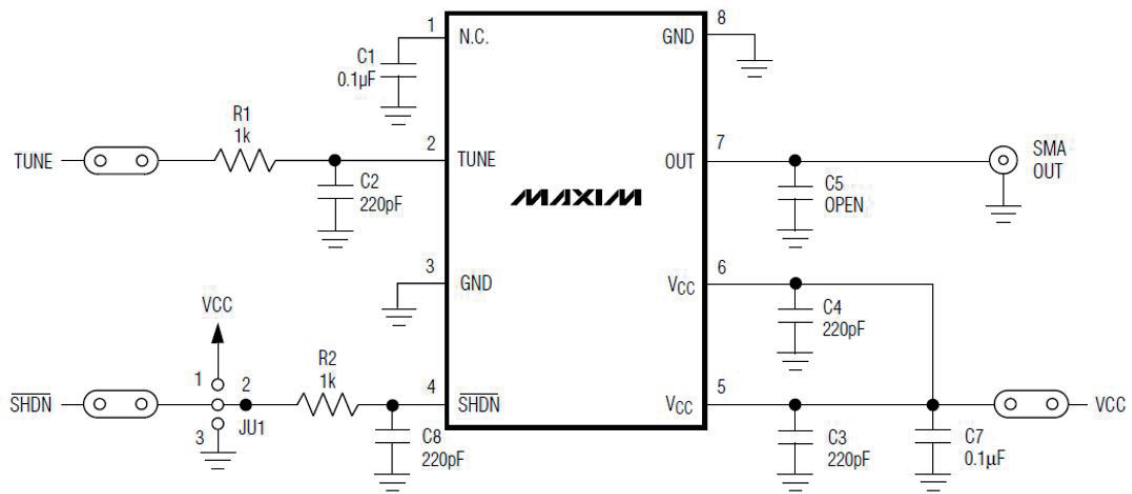
In the following subsections, we introduce the design and implementation of each module of the system.

2.1 RF signal generator implementation

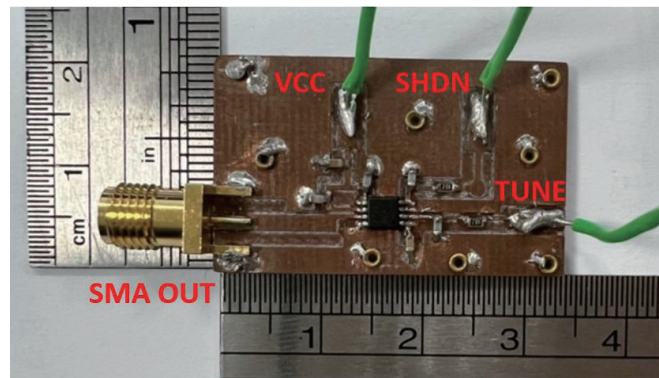
The RF signal generator is used to generate the stable high-frequency signal required by the system. In this study, the voltage-controlled oscillator (VCO) (model: MAX2750)⁽¹⁸⁾ is used as an RF signal generator, and the VCO circuit is shown in Fig. 2(a). As shown in the figure, the pin descriptions of the VCO are as follows: VCC is the DC supply voltage; TUNE is the oscillator frequency tuning voltage input, which controls the output signal frequency; SHDN is the enable logic input, which can start or shut down the module operation; SMA OUT is the RF signal output. The VCO circuit is implemented and its photograph is shown in Fig. 2(b). When the VCC and SHDN pins are both biased at 3 V, and the TUNE pin is biased at 0.96 V, the VCO module will generate a 2.4 GHz signal at the SMA OUT pin. We utilized a spectrum analyzer (model: Anritsu MS2035B) to measure the output signal, and it shows that the output signal is at 2.4 GHz with -2.34 dBm power as shown in Fig. 3. The measured results show that this output signal has low noise and stable characteristics, and that the signal power is large enough, making it a suitable signal source for a sensing system.

2.2 BGL sensor element design and implementation

Omer *et al.* used the lump element model of a microstrip line with a four-cell CSRR hexagonal configuration to explain the detection mechanism of the BGL sensor.⁽¹⁶⁾ On the basis of the detection mechanism, we design a unique BGL sensor using a metamaterials technique as shown in Fig. 4(a). This sensor is implemented on a double-layer printed circuit board (PCB). The upper metal is a metamaterial cell array,^(19–21) the middle insulation material is a 0.8-mm-thick FR4 dielectric substrate (relative permittivity $\epsilon_r = 4.4$), and the lower metal is a transmission line (TL). The proposed sensor utilizes a metamaterial cell array to improve the sensing sensitivity. When a blood glucose sample is placed on the sensor, the sample changes the equivalent relative permittivity of the substrate, varying the frequency response of the sensor



(a)



(b)

Fig. 2. (Color online) (a) MAX2750 evaluation board schematic.⁽¹⁸⁾ (b) Photograph of MAX2750 module.

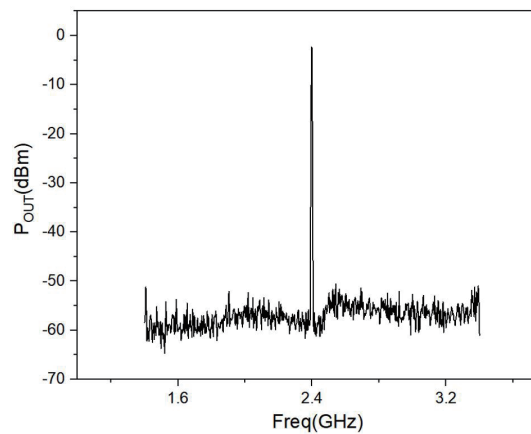


Fig. 3. Measured frequency response of VCO output RF signal.

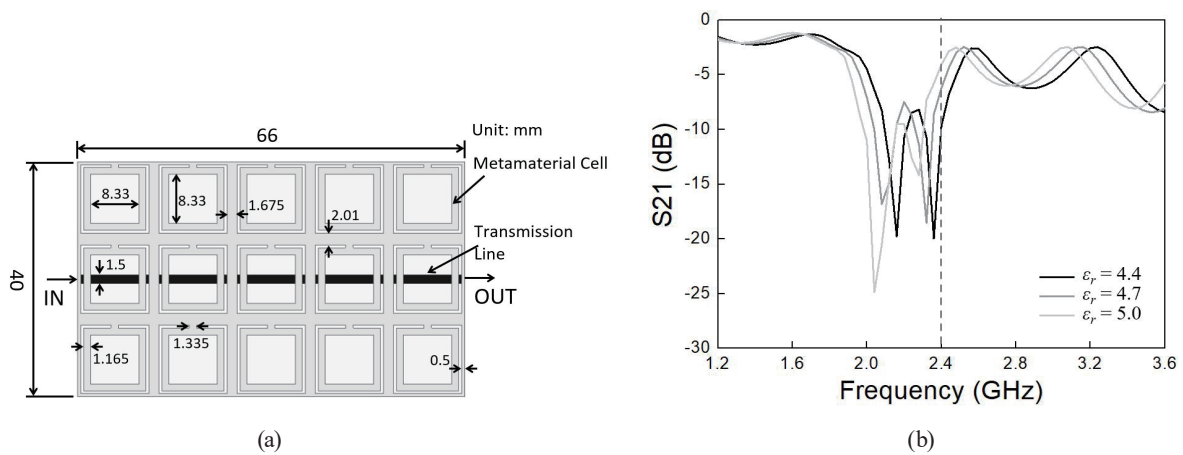


Fig. 4. (a) Configuration of proposed sensor element. (b) S_{21} frequency response performance of TL.

output signal. Then, we can obtain the method for measuring BGL through the corresponding relationship between the variation of the signal frequency response and BGL.

We use electromagnetic (EM) simulation software to design the proposed sensor and to simulate its S_{21} frequency response, as shown in Fig. 4(b) with the black line. S_{21} is the ratio of the input signal wave to the output signal wave in the decibel scale, and the S_{21} frequency response shows a large loss in the frequency range from 2.1 to 2.4 GHz because the metamaterial cells resonate in this frequency region. This resonance of the cells can be observed through the simulated electric field distribution at 2.35 GHz as shown in Fig. 5(a), because the electric fields are in the high range in most regions. Figure 5(b) shows a photograph of the sensor element.

Moreover, in order to understand the effect of blood glucose samples with different glucose levels on the equivalent relative dielectric constant of the substrate, the S_{21} characteristics of the sensor with various equivalent relative permittivities of the substrate are simulated as shown in Fig. 4(b). The figure shows that the S_{21} frequency responses of the sensor element shift to a lower frequency with increasing relative permittivity. When the frequency is fixed at 2.4 GHz as shown in the figure with the dotted line, the S_{21} magnitude increases with the relative permittivity, which indicates that the S_{21} magnitude can correspond to BGL when the sensor element operates at a fixed frequency.

2.3 RF-DC rectifier design and implementation

The RF-DC rectifier is one of the important circuits in the BGL sensor system, which can convert the RF signal into a suitable DC supply voltage. In this study, the Cockcroft–Walton multiplier⁽²²⁾ is used in the RF rectifier to boost the output DC voltage to improve the sensor sensitivity. The design method of the circuit is introduced in Ref. 23.

We use an electronic circuit simulator to design a six-stage Cockcroft–Walton voltage multiplier circuit schematic as shown in Fig. 6(a), and the layout of the circuit is shown in Fig. 6(b). The substrate of the circuit is a 0.8-mm-thick PCB with a relative permittivity of 4.4 and a loss tangent of 0.02. The solid-line rectangles indicate the locations of the SMS7630 Schottky diodes.⁽²⁴⁾ The size parameters of the layout are listed in Table 1.

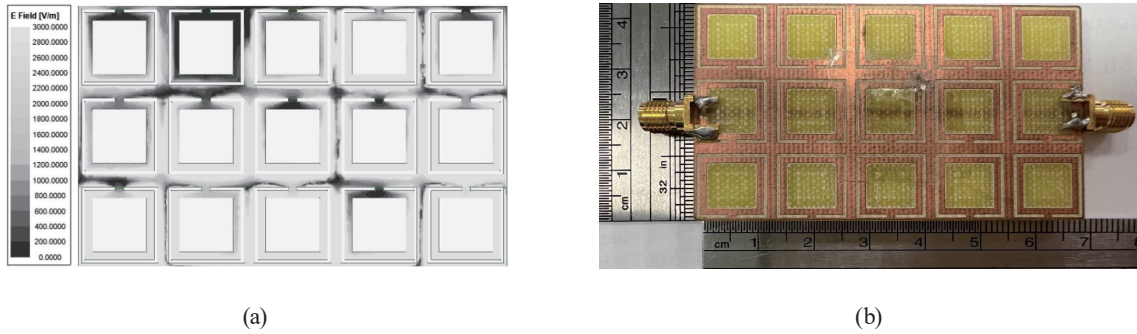


Fig. 5. (Color online) (a) Simulated electric field distribution of sensor element at 2.35 GHz. (b) Photograph of sensor element.

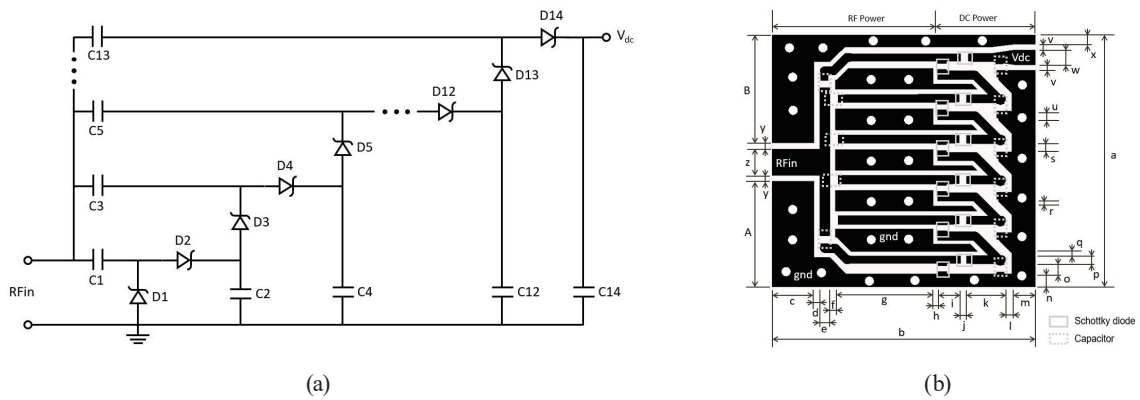


Fig. 6. (a) RF-DC rectifier schematic. (b) RF-DC rectifier layout.

Table 1
Size parameters of 10-stage RF rectifier.

Dimension	a	b	c	d	e	f	g	h
Size (mm)	28.6	29.9	4.8	0.61	1.2	1.82	10.38	1.05
Dimension	i	j	k	l	m	n	o	p
Size (mm)	1.56	0.64	4.3	0.85	2.7	1.5	1	0.9
Dimension	q	r	s	t	u	v	w	x
Size (mm)	0.38	0.38	0.98	0.5	1	0.62	1.7	1.1
Dimension	y	z	A	B				
Size (mm)	0.64	3	12	12.3				

The RF-DC rectifier is implemented and the photograph of the circuit is shown in Fig. 7. A VNA (model: Anritsu MS46122B) is utilized to measure the reflection coefficient (S_{11}) frequency response as shown in Fig. 8(a). The results show that S_{11} is lower than -10 dB at 2.4 GHz, which indicates that the rectifier can operate at 2.4 GHz. A radio frequency signal generator (model: Agilent E34483C) is utilized to generate a high-frequency signal, and the signal power is imported to the circuit to convert an output DC voltage. Figure 8(b) shows the relationship between the output DC output voltage (V_{dc}) and the RF input signal power (P_{in}) when the circuit output is connected to a 7.9 k Ω load.

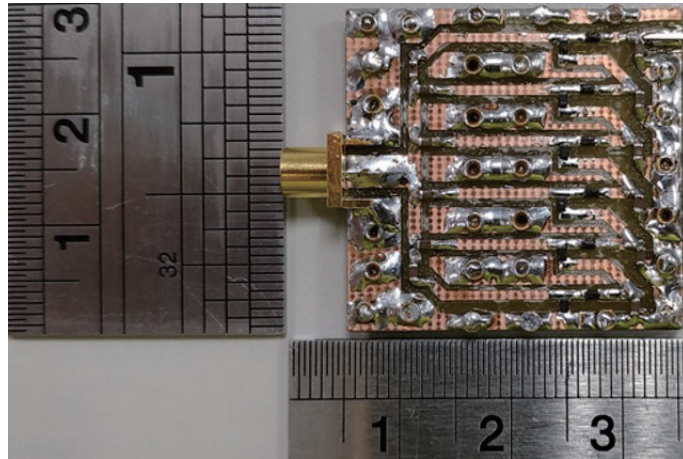


Fig. 7. (Color online) Photograph of RF-DC rectifier.

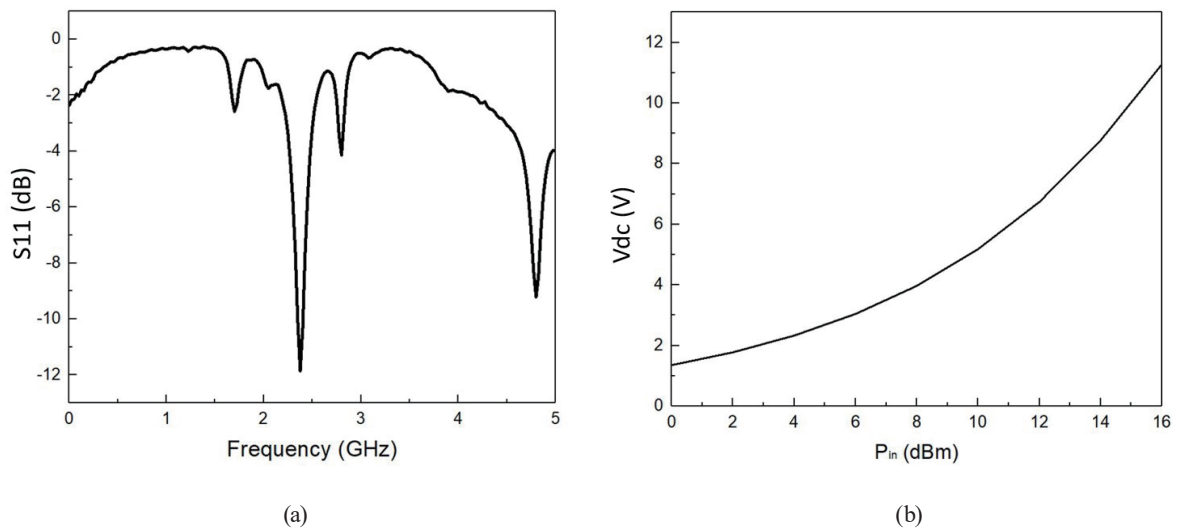


Fig. 8. (a) S₁₁ frequency response performance of RF-DC rectifier. (b) Relationship curve between output DC voltage of RF-DC rectifier and input signal power.

2.4 Amplifier module

In this study, the amplifier module in the system is used to amplify the sensing signal from the output of the RF-DC rectifier so that the sensing signal can be analyzed and calculated more easily. Figure 9(a) shows a photograph of the amplifier module. The operation bias voltage of this module is 24 V, and the voltage gain can be adjusted by the variable resistor. The maximum output voltage can reach 10 V, and the module size is $4 \times 3 \text{ cm}^2$. In this study, the voltage gain of the amplifying module is adjusted to 3.01 as shown in Fig. 9(b).

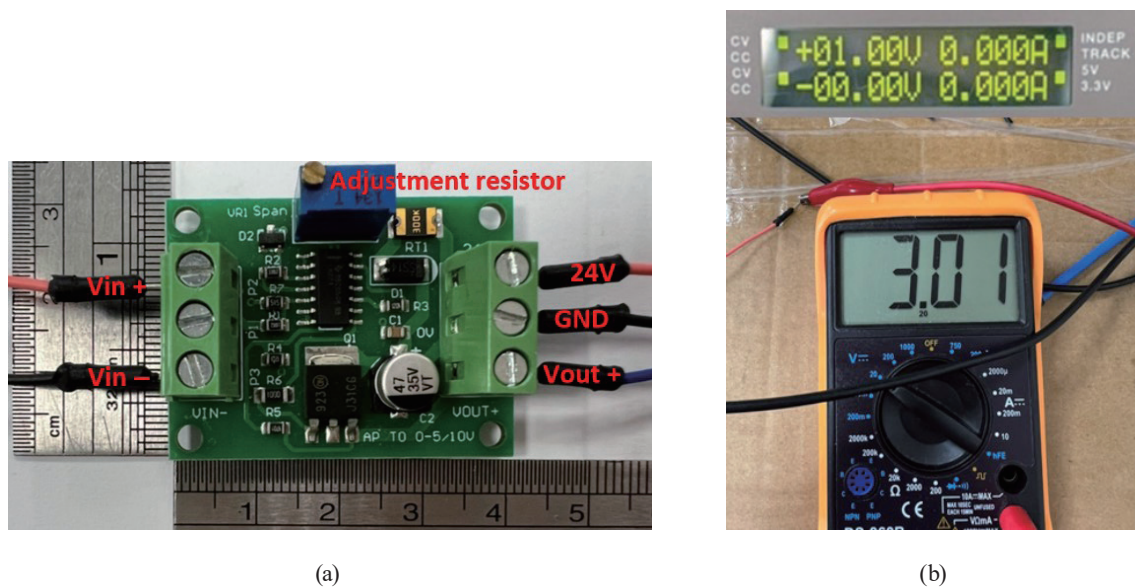


Fig. 9. (Color online) (a) Photograph of amplifier module. (b) Adjusting the amplifier gain using a 1 V input voltage.

2.5 Embedded system

The embedded system (model: Arduino Nano), as shown in Fig. 10, is used to read the sensing voltage by the amplifier. Then, the microcontroller (MCU) calculates the BGL corresponding to the sensing voltage and displays the calculated BGL on the LCD screen. The Arduino Nano size is small ($40.6 \times 17.7 \text{ mm}^2$), and the module uses the ATmega8 produced by Atmel Corporation.⁽²⁵⁾ The BGL algorithm is introduced in the next section.

3. System Integration

We integrate a VCO, a sensor, an RF-DC circuit, an amplifier module, embedded systems, and a screen into a noninvasive BGL sensor, as shown in Fig. 11. There are two steps to perform in order for the system to sense BGL in the fingertip. The first step is to obtain the corresponding curve relationship between the glucose concentration and the sensing voltage, as shown by the black curves in Fig. 12. The second step is calibration, which is to find the corresponding relationship between BGL in the fingertip and the sensing voltage, as shown by the gray points in Fig. 12, so that the relationship can be obtained to determine BGL in the fingertip from the sensing voltage.

For the first step, a container is placed on the sensor element as shown in Fig. 11, and samples of various glucose concentrations are dropped in the container. The embedded system is utilized to read the sensing voltage using the amplifier, which corresponds to the glucose sample. The corresponding characteristic curve between the glucose concentration and the sensing voltage can be obtained as shown by the black line in Fig. 13. Then, the fitting curve and the behavior

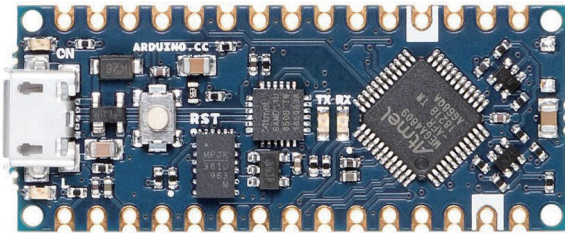


Fig. 10. (Color online) Photograph of Arduino Nano.

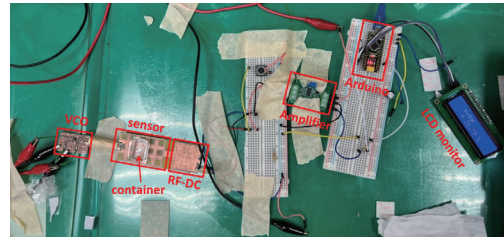


Fig. 11. (Color online) Photograph of Arduino Nano.

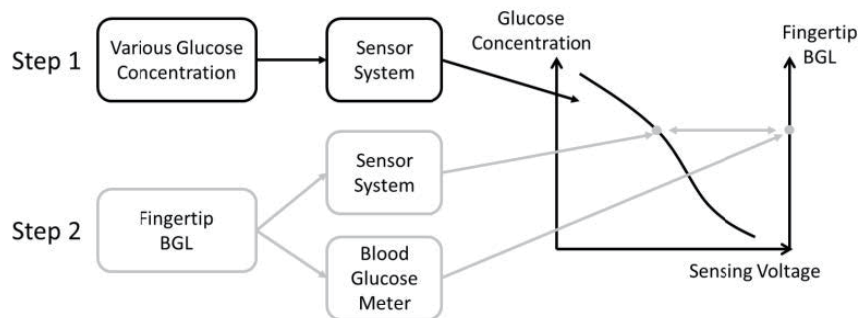


Fig. 12. The sensor system detects the BGL calculation steps.

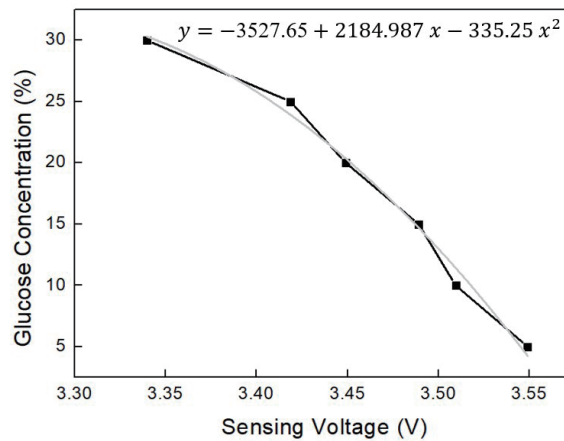


Fig. 13. Relationship curve between glucose concentration and sensing voltage.

equation of the characteristic curve between the glucose concentration and the sensing voltage are found, as shown by the gray line in Fig. 13. This behavior equation, expressed as Eq. (1), is a second-order polynomial, where the intercept parameter a_0 is -3527.65 , the first-order parameter a_1 is 2184.987 , and the second-order parameter a_3 is -335.25 .

$$y = a_0 + a_1x + a_2x^2 \quad (1)$$

Regarding the second step, we utilize a traditional invasive blood glucose meter (model: Contour Next ONE)⁽²⁶⁾ for sensor calibration. The calibration method involves the use of the invasive blood glucose meter and the proposed noninvasive BGL sensor to measure human blood glucose under the same situation. As shown in Fig. 12, the measurement value (point B) of the noninvasive sensing system is adjusted to the test value (point A) of the invasive blood glucose meter by shifting the relationship curve [modified a_0 in Eq. (1)]. For more effective calibration, we averaged the BGLs obtained before and after meals for 15 times, and the average pre-meal and post-meal BGLs measured using the proposed sensor system are 96.66 and 122.87 mg/dL, respectively. Note that the post-meal measurement is performed within 3 min after eating. After sensor calibration, the post-meal BGLs detected using the blood glucose meter and the proposed BGL sensor are 121 and 122.87 mg/dL, respectively, as shown in Fig. 14. The error between the detections is 1.55%.

All the modules of the system are integrated in a $12 \times 17 \times 8$ cm³ case. Figure 15(a) is a photograph of the interior of the sensing system, Fig. 15(b) shows the appearance of the sensing system, and Fig. 15(c) is the operating condition of the system. The advantages of the proposed sensor are noninvasive testing, small size, light weight, easy to carry, reusability, and low power consumption.

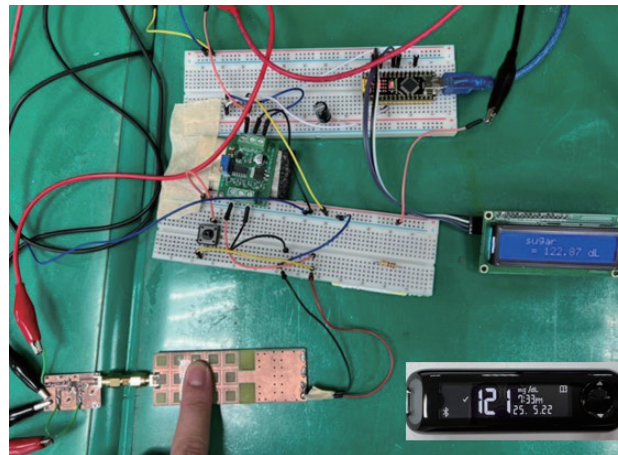


Fig. 14. (Color online) Comparison of post-meal BGLs measured using blood glucose meter and proposed sensor.

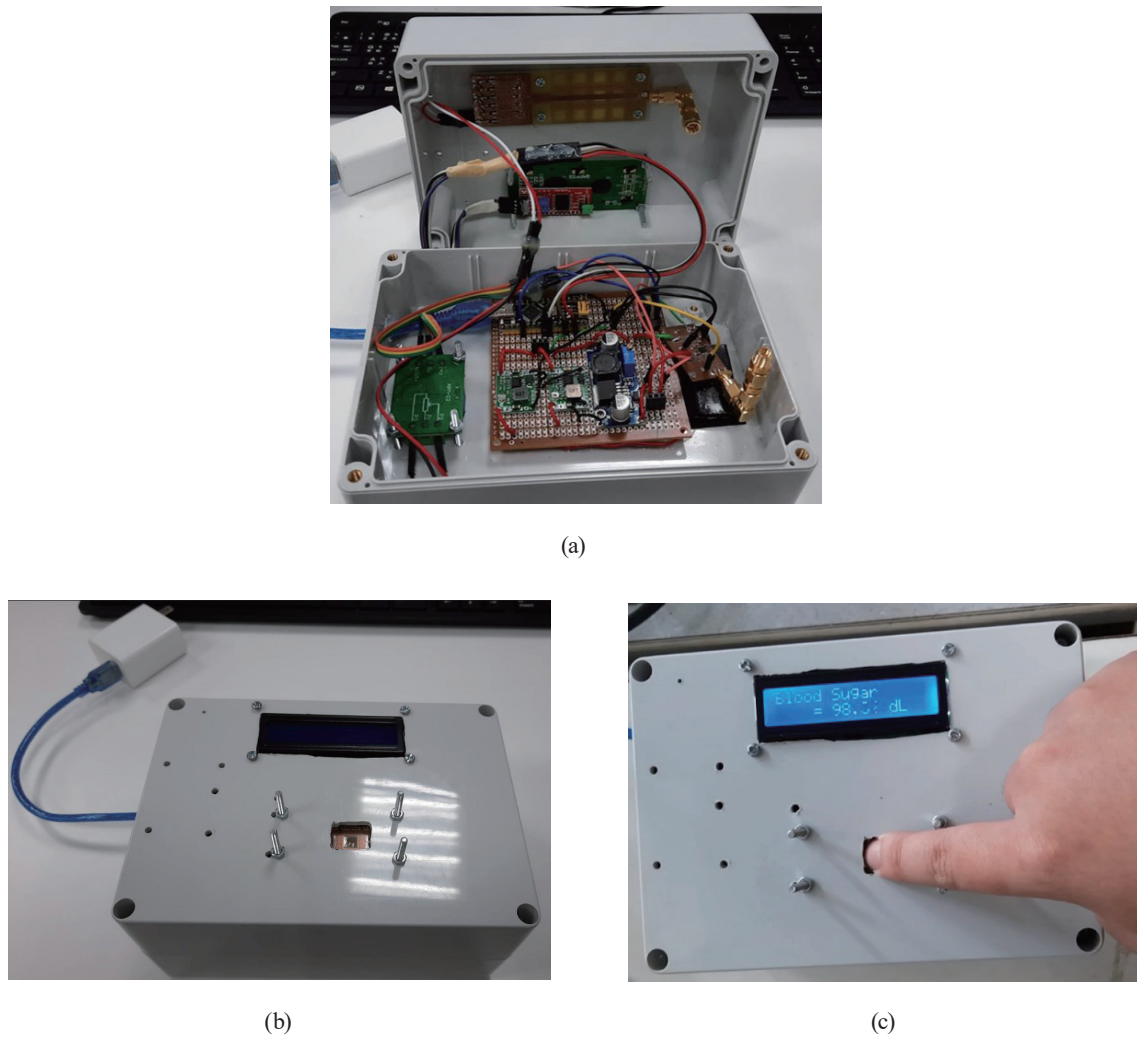


Fig. 15. (Color online) (a) Photograph of proposed sensor system device interior. (b) Sensor system appearance. (c) Operation situation in which sensing system is in use.

4. Conclusions

In this study, a cost-effective noninvasive 2.4 GHz microwave blood glucose sensor is developed and implemented. A special sensing element with metamaterials was designed and implemented for the sensitive sensing of changes in glucose concentration. A 2.4 GHz RF-DC rectifier circuit is also designed for the sensor, which converts the sensing signal from an RF signal to DC voltage. An algorithm that can calculate BGL from the sensing voltage is developed and programmed to run in the embedded system. All the modules of the system are integrated in a small case of $12 \times 17 \times 8 \text{ cm}^3$ size. This system can work independently and does not require the integration of other equipment. Compared with invasive blood glucose meters, the detection error of the sensor is less than 2%. The proposed sensor is light, small, easy to carry, and inexpensive. It is suitable as one of the options for noninvasive blood glucose test solutions.

References

- 1 International Diabetes Federation (IDF): <https://idf.org/about-diabetes/facts-figures/> (accessed August 2023).
- 2 T. Lin, A. Gal, Y. Mayzel, K. Horman, and K. Bahartan: *Curr. Trends Biomed. Eng. Biosci.* **6** (2017) 1.
- 3 D. Bruen, C. Delaney, L. Florea, and D. Diamond: *Sensors* **7** (2017) 1866.
- 4 J. P. Comer: *Anal. Chem.* **28** (1956) 1748.
- 5 H. Yao, A. J. Shum, M. Cowan, I. Lähdesmäki, and B. A. Parviz: *Biosens. Bioelectron.* **26** (2011) 3290.
- 6 A. Siegel, R. H. Guy, and M. B. Delgado-Charro: *Clin. Chem.* **50** (2004) 1383.
- 7 A. Caduff, M. S. Talary, M. Mueller, F. Dewarrat, J. Klisic, M. Donath, L. Heinemann, and W. A. Stahel: *Biosens. Bioelectron.* **24** (2009) 2778.
- 8 J. Kost, M. Pishko, R. A. Gabbay, R. Langer, and S. Mitragotri: *Nat. Med.* **6** (2000) 347.
- 9 S. Kiani, P. Rezaei, M. Karami, and R. A. Sadeghzadeh: *IET Wireless Sens. Syst.* **9** (2019) 1.
- 10 T. Yilmaz, R. Foster, and Y. Hao: *Diagnostics* **9** (2019) 6.
- 11 S. Saha, H. Cano-Garcia, I. Sotiriou, O. Lipscombe, I. Gouzouasis, M. Koutsoupidou, G. Palikaras, R. Mackenzie, T. Reeve, P. Kosmas, and E. Kallos: *Sci. Rep.* **7** (2017) 6855.
- 12 M. Bteich, J. Hanna, J. Costantine, R. Kanj, Y. Tawk, A. H. Ramadan, A. A. Eid: *IEEE J. Electromagn. RF Microwaves Med. Biol.* **5** (2021) 139.
- 13 V. Turgul and I. Kale: *IEEE Sens. J.* **17** (2017) 7553.
- 14 S. Harnsoongnoen and A. Wanthong: *IEEE Sens. J.* **17** (2017) 1635.
- 15 M. Hofmann, M. Bloss, R. Weigel, G. Fischer, and D. Kissinger: *Proc. 42nd European Microwave Conf. (Amsterdam, Netherlands, 2012)* 546–549.
- 16 A. E. Omer, G. Shaker, S. Safavi-Naeini, H. Kokabi, G. Alquié, F. Deshours, and R. M. Shubair: *Sci. Rep.* **10** (2020) 15200.
- 17 I. E. Gelosi, R. Avalos Ribas, A. J. Uriz, J. Castiñeira Moreira, and N. Fuentes: *IEEE Lat. Am. Trans.* **20** (2022) 813.
- 18 Maxim MAX2750 datasheet: <https://datasheets.maximintegrated.com> (accessed August 2023).
- 19 D. R. Smith, J. B. Pendry, and M. C. K. Wiltshire: *Science* **305** (2004) 788.
- 20 A. Sanada, C. Caloz, and T. Itoh: *IEEE Microwave Wireless Compon. Lett.* **14** (2004) 68.
- 21 S. N. Burokur, M. Latrach, and S. Toutain: *J. Electromagn. Waves Appl.* **19** (2005) 1407.
- 22 J. D. Cockcroft and E. T. S. Walton: *Proc. R. Soc. A* **137** (1932) 229. <https://doi.org/10.1098/rspa.1932.0133>.
- 23 Ja-Hao Chen, Yu-Chang Lin, Tai-Chieh Tseng, and Cheng-Chi Yu: *Sens. Mater.* **35** (2023) 1599.
- 24 SMS7630 Schottky diodes data sheet: https://www.skyworksinc.com/-/media/SkyWorks/Documents/Products/201-300/Surface_Mount_Schottky_Diodes_200041AG.pdf (accessed August 2023).
- 25 ATmega8 datasheet: https://ww1.microchip.com/downloads/en/DeviceDoc/Atmel-2486-8-bit-AVR-microcontroller-ATmega8_L_datasheet.pdf (accessed August 2023).
- 26 Contour Next ONE: <https://www.ascensiadiabetes.com/products/contour-next-one/> (accessed August 2023).

About the Authors



Ja-Hao Chen received his B.S. degree in electronics engineering from Fu-Jen University, Taipei, Taiwan, in 1997 and his Ph.D. degree in electrical engineering from National Cheng Kung University, Tainan, Taiwan, in 2002. From 2002 to 2005, he was with ALi Corporation, Taipei, Taiwan, where he worked on on-chip analog and digital I/O pads and ESD protection circuit design. From 2005 to 2007, he was with RichWave, Taipei, Taiwan, where he worked on on-chip RF power amplifiers and RF switch circuit design. From 2007 to 2012, he was with the Department of Electrical Engineering, Tunghai University, Taichung, Taiwan, as an assistant professor. He is currently an associate professor in the Department of Communication Engineering, Feng-Chia University, Taichung, Taiwan. His research interests include on-chip RF circuit design and antennas for sensor and wireless power transfer applications. (chiahaoc@fcu.edu.tw)



Keng-I Lai received his M.S. degree in communication engineering from Feng-Chia University, Taichung, Taiwan, in 2022. His research interests include RF circuit design and metamaterials for blood glucose sensor applications. (andy525966@gmail.com)